Optics and Lasers in Engineering 51 (2013) 1245–1254

Contents lists available at SciVerse ScienceDirect

Optics and Lasers in Engineering

journal homepage: www.elsevier.com/locate/optlaseng

Simulation and optimization of continuous laser transmission welding between PET and titanium through FEM, RSM, GA and experiments

Xiao Wang *, Hao Chen, Huixia Liu, Pin Li, Zhang Yan, Chuang Huang, Zhenuan Zhao, Yuxuan Gu

School of Mechanical Engineering, Jiangsu University, Zhenjiang 212013, China

ARTICLE INFO

Article history:
Received 31 December 2012
Received in revised form
12 March 2013
Accepted 30 April 2013
Available online 30 May 2013

Keywords:
Continuous laser transmission welding (LTW)
Finite element method (FEM)
Response surface methodology (RSM)
Genetic algorithum(GA)

ABSTRACT

An intelligent method for simulation and optimization of continuous laser transmission welding (LTW) and validated with experiments (EX) is investigated in this paper. Thermal model using finite element method (FEM) has been combined with response surface methodology (RSM) and genetic algorithm (GA) techniques to improve veracity of the model prediction with less time spending on the experiments. A three-dimensional axi-symmetric thermal model has been developed to simulate the continuous LTW process with a moving Super-Gaussian heat source. The model is confirmed with a series of experiments. A statistical technique RSM based mathematical model is proposed to establish relations between input variables (*power, welding speed, stand-off-distance*) and output variables (maximum temperature at the weld interface-T_{max}, maximum temperature at the top surface of the transparent PET-T_{top}, weld width-*WW*, and weld depth in the transparent PET-*DT*). The RSM models are trained and tested by using the data from the numerical (FEM) models. It turns out that the models are proposed to accurately predict the output variables with the corresponding input variables. Finally, the desirability function (DF) integrated with the developed non-dominating sorting genetic algorithm-II (NSGA-II) is used to find out the optimal variables that enhance the quality and efficiency of the welding. Experiments using the optimum parameters are carried out to verify the FEM and RSM models. Results show that the proposed integrated (FEM–RSM–GA–EX) approach performed very well in optimum performance of the continuous LTW process. In addition, this approach also presents the feasibility of the use of the FE simulation to guide the experiments.

1. Introduction

Laser transmission welding (LTW) is a widely promising application technology with a lot of advantages, such as non-contact, non- pollution, high welding speed, accuracy, flexibility, easy to manipulate and so on [1]. In this process, the moving laser beam passes through the upper transparent material and then penetrates on the opaque surface of the lower material. In other words, firstly, the thermal energy absorbed by the opaque part produces the heat at the weld interface of both materials. Afterwards, the opaque part will heat up and this heating can cause the two materials to be softened at the weld interface. Finally, a joining area is formed between the two materials.

In an early time, with the development of numerical methods viz. RSM, GA, ANN, etc, which are widely used in modeling and optimizing the performance of the manufacturing technologies, researchers use experiment data, are concentrating on developing numerical models to predict and optimize the process capabilities and weld characteristics accurately. Wang et al. [2] developed mathematical models between joining parameters and desired responses using response surface methodology (RSM). Then the models were used to optimize the process parameters of laser transmission welding. The predicted values from mathematical models nearly agreed with the experiment values, which showed that the models could predict the responses adequately and optimize the process parameters efficiently. Using response surface methodology, the model and optimization between process parameters and desired responses of laser transmission welding process were studied by Liu et al. [1]. The results indicated that the optimal process parameters were 11.2 W, 4 mm/s and 163 nm, respectively. Acherjee et al. [3] developed RSM models of the LTW process and discussed the interaction effects of process parameters on the responses. Wang et al. [4] developed mathematical models of LTW process using RSM and GA for prediction of weld width and weld strength. GA was used to optimize the output process parameters.

Though using the above methods could predict the weld characteristics of the LTW process accurately, LTW processing

* Corresponding author. Tel.: +86 511 88797998; fax: +86 511 88780276.
E-mail address: wx@ujs.edu.cn (X. Wang).

0143-8166/$ - see front matter © 2013 Elsevier Ltd. All rights reserved.
http://dx.doi.org/10.1016/j.optlaseng.2013.04.021

experiments for investigating different aspects of the process are a time-consuming and costly work, on the other hand, with the popularization of computers, also with the evolution of finite element methods (FEM), more and more researchers are choosing FEM which reduce the experimental time and cost to simulate LTW process with acceptable accuracy. The biggest benefits of using finite element methods are to provide guidance for experiments and improve efficiency and quality of the LTW process. Researchers, of late, are attempted to develop the model of temperature field and interrelated weld width, weld penetration depth, etc. in LTW process. Boglea et al. [5] set a one-dimensional heat transfer model and compared the calculated values with experiment data of weld width. A two-dimensional finite element model of LTW process was presented by Prabhakaran et al. [6] for glass reinforced nylon 6. The transient temperature distribution obtained from the model was compared with experimental observations, which achieved good agreement. Mayboudi and Birk [7] set a two-dimensional thermal finite element model of laser transmission welding for T joint. The 2D model was used to predict the molten zone depth as well as the transient temperature distribution along the weld line. Mahmood and Mian [8] presented a FE model to determine the optimum parameters of jointing two dissimilar materials viz. polyimide and titanium. For a particular value of the laser power, good bonding at the weld interface of the two materials is a function of laser welding speed. Mian and Mahmood [9] studied the laser irradiated joints between glass and polyimide, three dimensional uncoupled finite element model was conducted to investigate the effect of variational process parameters in bond quality. Acherjee et al. [10] developed a three-dimensional thermal model to simulate the LTW process between polyvinylidene fluoride and titanium. In recent years, although some researchers used numerical methods or finite element methods alone to study the LTW process, few people combined the two methodologies. It is an imminent problem and individual people did this research. Acherjee et al. [11] developed a three-dimensional thermal model to simulate the laser transmission contour welding process. Mathematical models, based on simulation results, were developed to analyze the process. Sensitivity analysis was performed to study the relative influence of different parameters on the output parameters. Acherjee et al. [12] modeled and analysed the simultaneous laser welding of polycarbonates with an FEM–RSM integrated approach. The mathematical models were further used for selecting the optimal process parameters to obtain an acceptable welding, however, it only gave graphical optimization results which failed to get down to specific.

Review of past literatures, some of the studies devote to the development of mathematical models for predicting the weld strength and weld width, others devote to thermal models for predicting the temperature field, it can be seen that no efficient, comprehensive approach is made to model the LTW process so far has been reported to study and predict welding characteristics accurately during LTW process, and use it further to obtain the optimal process parameters. Unlike Dr Acherjee's research of laser transmission contour welding process and simultaneous laser transmission welding process, this article studies continuous laser transmission welding process. The materials used in this study are 0.1 mm thick PET (polyethylene terephthalate) films and 0.035 mm thick titanium foil and welded by means of a continuous wave radiation with a near infrared diode laser. The two materials are biocompatible materials and can be joined as implantable Microsystems to adapt complicated biological, physical and chemical environments in the human body.

In this work, in order to reduce the experimental time and cost, a numerical study has been carried out to simulate and optimize the continuous laser transmission welding through a comprehensive and integrated (FEM–RSM–GA–EX) approach. In this approach, FEM is used to develop the thermal model, RSM is applied to design the experiments and develop the mathematical models based on simulation results, GA which is applied to obtain a set of optimal process parameters in this study represents desirability function (DF) and non-dominating sorting genetic algorithm-II (NSGA-II). EX (experiments) is conducted to validate the reliability of the models.

Fig. 1 shows the proposed approach for continuous LTW process using FEM, RSM, GA and EX. It mainly includes three steps: (1) to develop an axi-symmetric thermal model and validated with experimental results; (2) to establish RSM models and tested by using the data from the numerical models; (3) to select the optimum process parameters using desirability function (DF) and non-dominating sorting genetic algorithm-II (NSGA-II), which confirmed with experimental results, RSM models and simulated data.

2. Thermal model of LTW using FEM

Fig. 2 shows the schematic diagram of the continuous laser transmission welding process with lap joint used in this work.

The actual dimension of the sample and one half of the lapped portion with symmetric molten zone that is available are presented in Fig. 3.

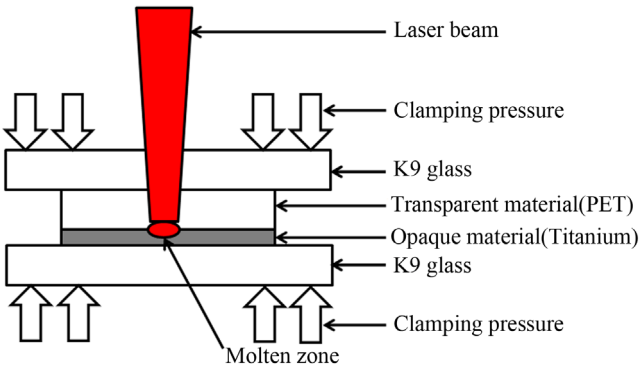

Fig. 2. Schematic of continuous laser transmission welding process.

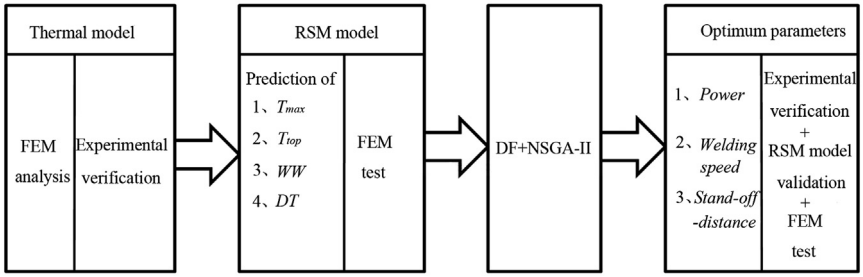

Fig. 1. LTW model development, optimization and verification approach.

In this study, a Copmact 130/140 semiconductor continuous laser manufactured by Dilas is used for the experiments. The maximum power of the laser device is 130 W, the output wavelength is 980 ± 10 nm, the core of the optical fiber is 400 nm and the numerical aperture is 0.22 μm. The same conditions of the experiments are used in this finite element simulation. Some assumptions are also made for simplifying the development of the numerical model, which are shown below [12]:

(1) Symmetry to simplify model geometry for reducing simulated time.
(2) A good contact between the welding materials.
(3) An isotropic thermal–physical behavior during welding.

2.1. Mathematical description of the thermal model

For uniform and continuous media, the spatial and temporal distribution of the temperature field fulfils the differential equation of three-dimensional heat conduction in a domain D, which is shown below [8]:

$$\frac{\partial}{\partial x}\left(k_x\frac{\partial T}{\partial x}\right)+\frac{\partial}{\partial y}\left(k_y\frac{\partial T}{\partial y}\right)+\frac{\partial}{\partial z}\left(k_z\frac{\partial T}{\partial z}\right)+Q=\rho c\left(\frac{\partial T}{\partial t}-v\frac{\partial T}{\partial x}\right) \quad (1)$$

where x, y, z are the coordinate values of the Cartesian coordinate system, T is the temperature (K), t is the time (s), ρ is the material density (kg/m^3), c is the specific heat capacity (J/(kg K)), k_x, k_y, k_z are the thermal conductivities in the x, y and z directions (W/(m K)), respectively, Q is the heat generation rate in per unit volume (W/(m K)) and v is the velocity of laser (m/s).

The initial condition can be written as:

$$T(x,y,z,0)=T_0 \quad (x,y,z)\in D \quad (2)$$

The natural boundary condition can be expressed as:

$$k_n\frac{\partial T}{\partial n}-q+h(T-T_0)+\sigma\varepsilon(T^4-T_0{}^4)=0 \quad (x,y,z)\in S \quad t>0 \quad (3)$$

where S represents the surfaces which are attached to imposed heat fluxes, radiation and convection, k_n is the thermal conductivity normal to Boundary S (W/(m K)), h is the coefficient of convection heat (W/(m^2 K)), σ is just a Stefan–Boltznann constant for radiation ($5.67\times10\text{E}{-8}$W/(m^{2}K^4)), ε is the heat radiation coefficient, T is the material surface temperature (K), T_0 is the initial temperature (K), q is the heat flux normal to Boundary S (W/m^2). Due to temperature-dependent thermo-physical properties (such as c, k) and thermal radiation conditions, this temperature field analysis becomes a typical nonlinear problem.

2.2. Numerical description of the thermal model

Laser transmission welding process is that parts of an area is quickly heated to high temperature and then rapidly cooled. Along with the movement of heat source, temperature rapidly changes with time and space in the whole workpiece process, and accompanying the changing of material thermal–physical properties, so a transient thermal analysis must be conducted. This requires a combination of the heat conduction equation based on time dependent. In the finite element analysis, this equation can be written as follows [13]:

$$[C(T)]\left\{\dot{T}\right\}+[K(T)]T=[Q(T)] \quad (4)$$

where $[K]$ is the conductivity matrix, including thermal conductivity coefficient, convection coefficient, radiation coefficient and shape coefficient, $[C]$ is the specific heat matrix, $\{T\}$ is the column vector of node temperature, $\{T^{\bullet}\}$ is the derivative of temperature versus time, $\{Q\}$ is the vector of nodal heat flow.

2.3. Modeling

For reducing the simulation time, a three-dimensional axisymmetric thermal model is developed by using finite element method (FEM) solver ANSYS 12.0, to calculate the distribution of temperature around the laser irradiated areas. The complete finite element analysis flow diagram is shown in Fig. 4.

Fig. 5 shows the finite element model in view of the effect of K9 glasses (4 mm thick) which are used as holding layers, the zone near the laser irradiated areas has been modeled with a finer mesh while the other zone has been modeled with a coarser one for reducing simulation time.

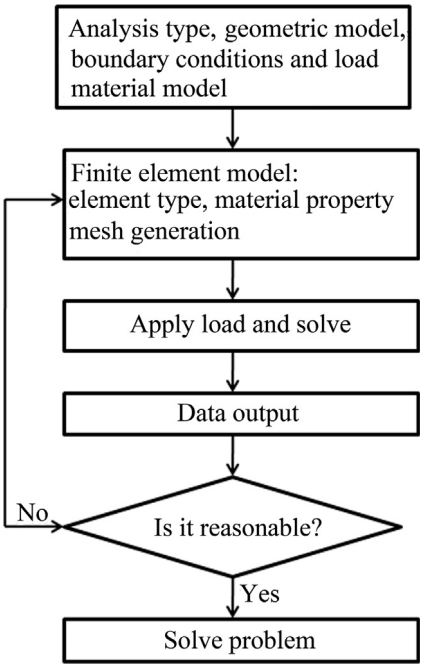

Fig. 4. Flow diagram of finite element analysis.

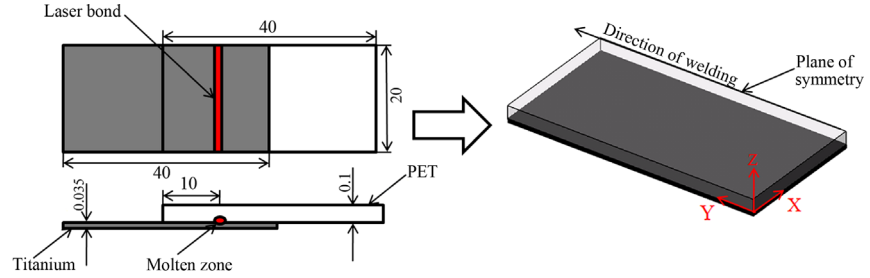

Fig. 3. Schematic of the sample dimension (numerical unit is mm) and one half of the lapped portion with symmetric molten zone.

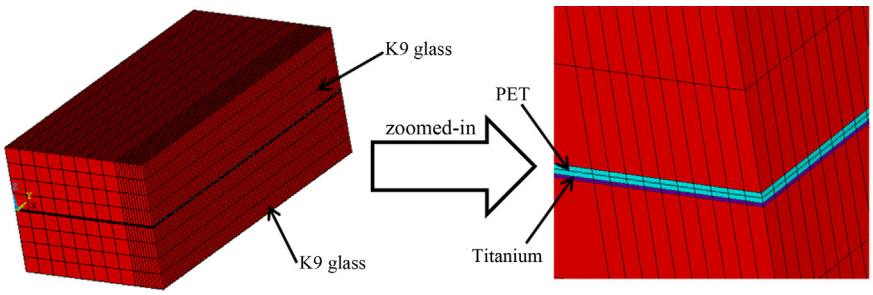

Fig. 5. Example of continuous laser transmission welding FE model and the zoomed-in mesh view near the weld interface.

Table 1
Thermal physical property parameters of the materials used in the FEM model.

Material	Density ρ (kg/m^3)	Specific heat C J/(kg K)	Thermal conductivity K W/(m K)
PET	1330	1100	0.35
Titanium	4510	530	17
K9 glass	2500	858	1.1

All three materials in the FE model viz. K9 glass, PET, and titanium, use SOLID 70 [14] element as thermal-brick elements, which owns only one temperature degree of freedom. In this case, material properties viz. density, thermal conductivity, specific heat [15] are employed in Table 1. For simplicity sake, changes in material properties depending on temperature during this continuous laser transmission welding process are not considered.

In this FE model, the fitting surfaces at the weld interface are modeled by two separate sets of nodes. Conduction, radiation and convection are taken account as the heat flow along with the welding direction. Convection coefficient is taken as 10 W/(m^3 K) and radiation coefficient is taken as 0.92. In this finite element model, the clamp pressure of 0.5 MPa is applied at the top surface of K9 glass to ensure the intimate contact between the welding materials. The moving super-Gaussian heat source whose energy is uniform Gaussian distribution is modeled as a distributed plane heat flux in the region near the laser irradiation areas. The distribution law of this heat flux is shown as follows [9]:

$$q(r)=\begin{cases} Q/(\pi r_b^2), & r\le r_b \\ 0, & r>r_b \end{cases} \quad (5)$$

where r_b is the laser facula radius (m), is the radius at which the heat flux intensity has decreased to 5% of its maximum heat flux density, r is the radial distance from the laser facula center and Q *is* the total energy of the absorption.

2.4. Results and discussion of temperature field analysis

Fig. 6 presents a contour plot of the transient temperature distribution acquired with the symmetry plane of the thermal model. In the view of this figure, the maximum temperature is 350 °C at the weld interface, which is far higher than fusion temperature, T_f (252 °C) of PET.

Fig. 7 shows the temperature contours at the *X–Z* plane, it can be seen that the thin titanium foil absorbs laser energy to produce high temperature. Allowing for the fusion temperature of PET, and in this simulation, the melting point of Titanium is 1660 °C, so no melting appears in the titanium foil. The region in Fig. 7 where temperature is above 252 °C shows the dimensions of weld width and melting depth in the transparent PET. Fig. 8 presents the calculated value of the melting depth.

The temperature distribution at the weld interface after 5 s is shown in Fig. 9. It can be observed that the isotherm contour of the fore-end is more intensive than the connection area and hysteretic temperature field comes after the laser moving trajectory. Considering the fusion temperature of PET, the weld half width (*WW*/2) is calculated with the data shown in Fig. 10. Fig. 11 shows the temperature distribution at the top surface of the transparent PET. It can be seen that PET thin film has an obvious thermal barrier effect and the temperature of the top surface has not reach the fusion temperature (252 °C). High quality welding can be available only when the temperature at the weld interface is above the fusion temperature (252 °C) but below the decomposition temperature (around 380 °C) of the PET, the temperature distribution at the top surface of the transparent PET should be below 252 °C, otherwise, the top surface will melt and cohere together with K9 glass, then the sample is damaged.

2.5. Validation of the thermal model with experiments

In the experiments, weld width and weld depth in the transparent PET are applied to verify the reliability of the thermal model. The macrograph and microgram of the welding sample chosen randomly from the experiments are shown in Fig. 12(a), (b) and (c). Fig. 13 shows the comparison results of simulative results and experiment data under different *powers*, *welding speeds* and *stand-off-distances*. It can be observed that the simulation results are in good agreement with the experiment data, in other words, the finite element model is reliable.

3. Design of experiments and mathematical modeling using RSM

3.1. Response surface method

As continuous LTW process is random and stochastic in nature and it is very difficult to predict the process responses accurately by mathematical equation, the RSM approach has been used in this study to model continuous LTW process and overcome these difficulties. One of advantages of using the RSM approach is that a model can be easily developed based on the given input parameters to accurately predict the output responses. This technique is especially significant in process where the relationship between process parameters is complex.

RSM is a combination of mathematical statistics and design of experiment that is used to model and analyze of problems in which a response of interest is restricted by several variables. The especial advantage of RSM is that it can reduce the number of experiments. The RSM uses low or high orders polynomial to estimate the response of a practical analysis code [16]. In this work, second-order polynomial

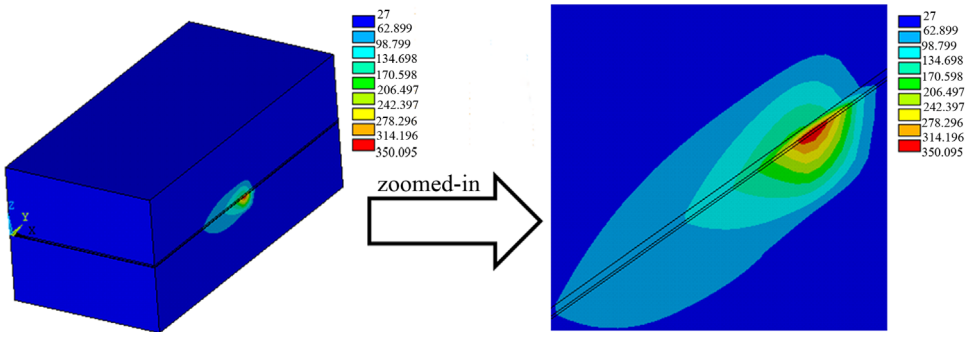

Fig. 6. Temperature contours at the symmetry plane (*Y–Z* plane) after 5 s (power=4.65 W, welding speed=2 mm/s and stand-off-distance=+3 mm).

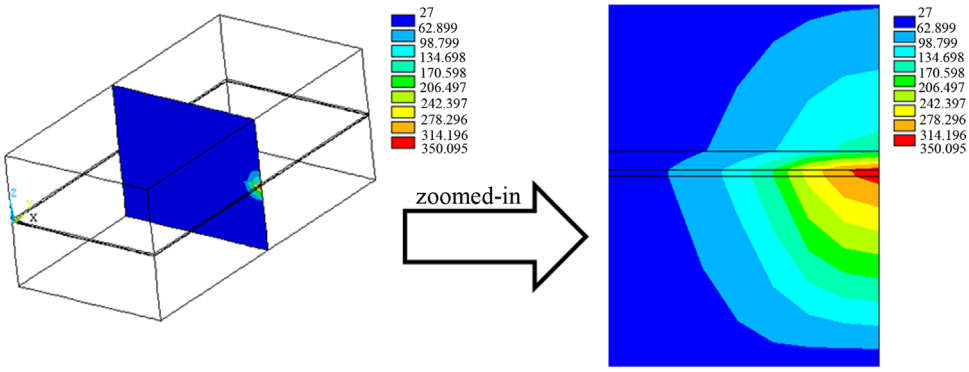

Fig. 7. Temperature contours at the *X–Z* plane after 5 s (power=4.65 W, welding speed=2 mm/s and stand-off-distance=+3 mm).

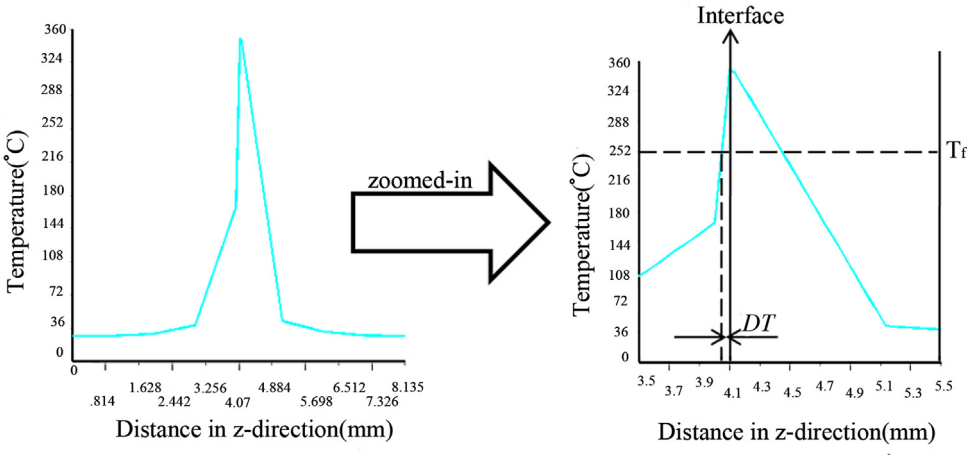

Fig. 8. Contour plot of temperature at the symmetry plane (*Y–Z* plane) after 5 s (*DT*=melting depth in transparent part, power=4.65 W, welding speed=2 mm/s and stand-off-distance=+3 mm).

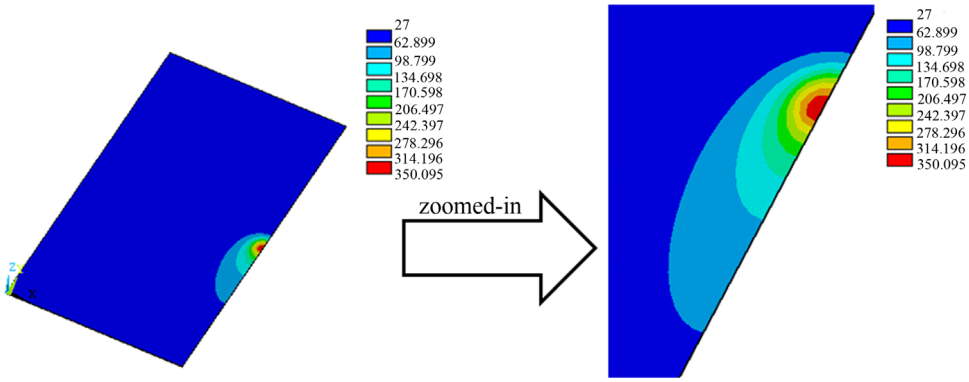

Fig. 9. Temperature contours at the symmetry plane (*X–Y* plane) after 5 s (power= 4.65 W, welding speed=2 mm/s and stand-off-distance=+3 mm).

is used with the following formulation:

$$y = \beta_0 + \sum_{j=1}^{k} \beta_j x_j + \sum_{j=1}^{k} \beta_{jj} x_j^2 + \sum_{i<j} \sum_{j=2}^{k} \beta_{ij} x_i x_j \quad (6)$$

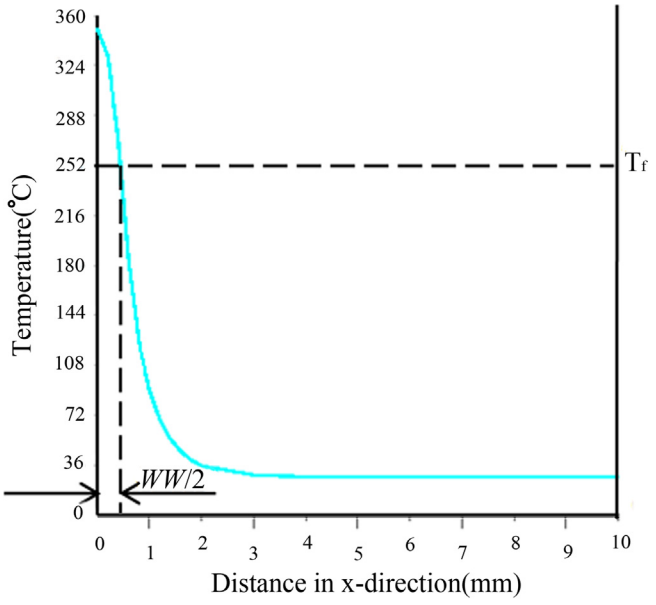

Fig. 10. Temperature distribution at the weld interface (*X*–*Y* plane) after 5 s (power=4.65 W, welding speed=2 mm/s and stand-off-distance=+3 mm).

where y is the response, k is the number of model inputs, x_i, x_j are called the set of model input variables (design variables), β_0, β_j, β_{jj}, β_{ij} are called the polynomial coefficients.

3.2. Experimental design

The experiments are designed based on a three-factor five-level central composite rotatable design, with full replication consisting of 2^3 factorial designs plus six center points and six star points. In this research, *laser power, welding speed* and *stand-off-distance* are the independently controllable process parameters of the continuous LTW process. The beam spot area is changing with the variational values of *stand-off-distance* viz. the distance between laser device and work material. The ranges and levels of experiment variables investigated in this study are given in Table 2. Four responses of interest, namely maximum temperature at the weld interface-T_{max}, maximum temperature at the top surface of the transparent PET-T_{top}, weld width-*WW*, and weld depth in the transparent PET-*DT*, are regarded as output variables. The central composite rotatable design matrix of the variables and the numerically simulated results of the different output variables are listed in Table 3. Statistical software Design-Expert v8 is used to code the variables and establish the design matrix.

3.3. Development of mathematical models

For responses of interest, the fit summary offers the quadratic model where the additional terms are significant and the model is not aliased [17]. The ANOVA analysis for the four response models are given in Table 4. It can be observed that the response models

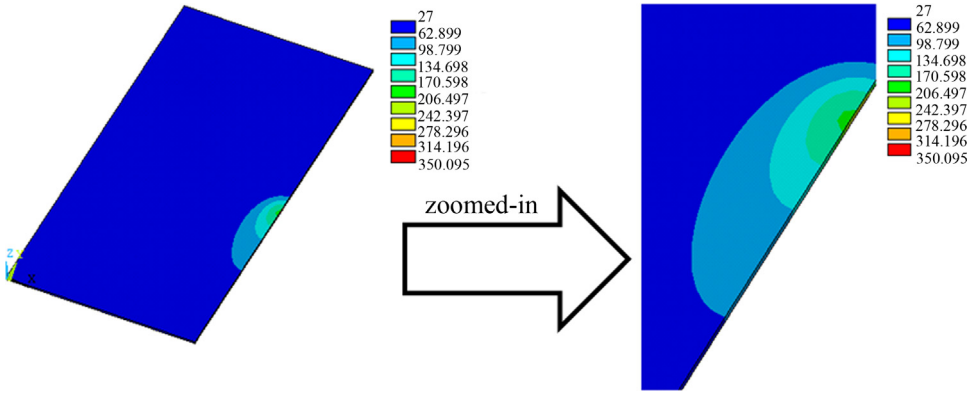

Fig. 11. Temperature distribution at the top surface of the transparent PET after 5 s (power=4.65 W, welding speed=2 mm/s and stand-off-distance=+3 mm).

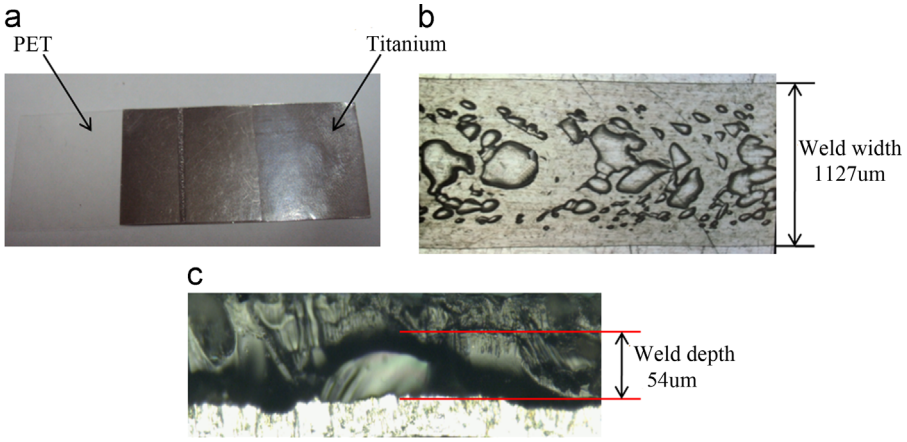

Fig. 12. (a) The macroscopic welding sample. (b) The microgram of the weld width. (c) The microgram of the weld depth.

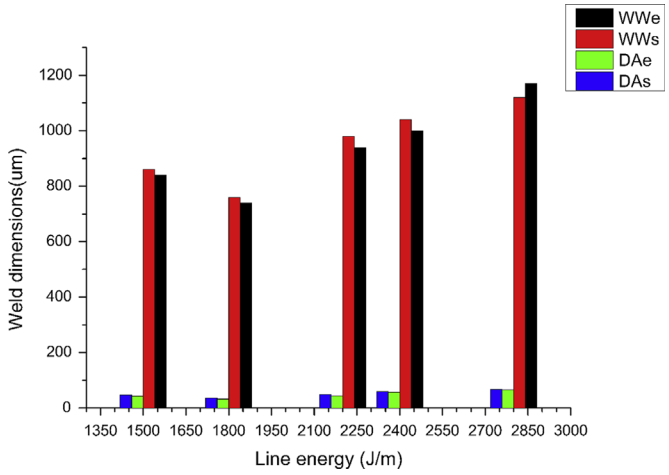

Fig. 13. Comparison of simulative results and experiment data under different powers, welding speeds and stand-off-distances.

Table 2
Process control parameters and their limits.

Parameters	Units	Notations	Limits				
			−2	−1	0	+1	+2
Power	W	*P*	4.1	4.65	6.1	7.55	8.1
Welding speed	mm/min	*S*	90	120	150	180	210
Stand-off-distance	mm	*F*	+2	+3	+4	+5	+6

Table 3
Design matrix and simulative responses.

No.	*P* (W)	*S* (mm/min)	*F* (mm)	T_{max}(°C)	T_{top} (°C)	*WW* (mm)	*DT* (mm)
1	6.10	150	+4.00	383.828	191.421	1.06	0.068
2	7.55	120	+5.00	475.429	258.251	1.45	–
3	7.55	180	+3.00	483.224	208.659	1.14	0.085
4	6.10	150	+2.00	503.904	212.541	1.19	0.088
5	4.65	180	+5.00	268.373	131.805	0.48	0.021
6	6.10	150	+6.00	328.923	173.864	1.11	0.051
7	6.10	150	+4.00	383.828	191.421	1.06	0.068
8	6.10	150	+4.00	383.828	191.421	1.06	0.068
9	6.10	210	+4.00	362.661	152.451	1.04	0.055
10	4.65	180	+3.00	307.986	125.986	0.68	0.035
11	4.65	120	+3.00	350.095	166.369	0.89	0.052
12	7.55	180	+5.00	418.907	197.168	1.26	0.082
13	6.10	150	+4.00	383.828	191.421	1.06	0.068
14	8.10	150	+4.00	500.821	223.125	1.36	0.092
15	6.10	90	+4.00	470.932	265.873	1.43	–
16	6.10	150	+4.00	383.828	191.421	1.06	0.068
17	6.10	150	+4.00	383.828	191.421	1.06	0.068
18	7.55	120	+3.00	551.599	253.289	1.32	–
19	4.10	150	+4.00	266.835	126.274	0.44	0.015
20	4.65	120	+5.00	303.185	169.427	0.84	0.045

are significant as the *p*-value is all less than 0.05. The adequate precision compares the signal-to-noise ratio and a ratio more than 4 is suitable [18]. The four values of adequate precision ratio which are all over 4 indicate that the models are adequate discrimination. The other adequacy measures of R^2 and adjusted R^2 are in reasonable agreement and are close to 1 [19], which indicate that the models are adequate and meaningful.

The final mathematical models determined by the Statistical software Design-Expert v8 are given as follows:

$$T_{max} = 376.45 + 112.43P - 80.57F - 2.92S - 4.65PF$$
$$-0.138PS + 0.08FS - 1.1P^2 + 7.61F^2 + 0.00856S^2$$

$$T_{top} = 14.3 + 91.58P + 7.33F - 1.665S - 1.33PF$$
$$-0.08PS - 0.057FS - 3.9P^2 + 0.58F^2 + 0.005S^2$$

$$WW = 1.111 + 0.5234P - 0.325F - 0.0178S + 0.0431PF$$
$$-0.047P^2 + 0.0191F^2 + 4.48e{-}5S^2$$

$$DT = 0.01336 + 0.0585P - 0.0164F - 1.425e{-}3S + 9.6e$$
$$-4PF - 4.85e{-}5PS - 1.31e{-}5FS - 2.864e{-}3P^2 + 7.43e$$
$$-4F^2 + 4.455e{-}6S^2$$

The models given above can be used to predict the maximum temperature at the weld interface (T_{max}), maximum temperature at the top surface of the transparent PET (T_{top}), weld width (*WW*), and depth of penetration in the transparent PET (*DT*), within the limited factors considered in this study.

3.4. Validation of the developed RSM models with simulated data

In order to validate the developed RSM models, three confirmation tests chosen randomly from the simulations are conducted with welding conditions chosen within the parameters space. The calculated values, predicted values and the percentage error of the RSM models verification are summarized in Table 5. From the validation tests, it can be obtained that the predicted error is very small between the calculated and the predicted values, which shows a good agreement between the developed RSM models and the FE models. Fig. 14((a)–(d)) shows the relationship between the calculated and predicted values of T_{max} (°C), T_{top} (°C), *WW* (mm) and *DT* (mm), respectively. It can be observed that there is a small percentage error between the calculated and predicted results, in other words, the developed models are adequate and the predicted values are in good agreement with the calculated values. Therefore, these mathematical models can be used for predicting the output variables of LTW process with significant accuracy.

4. Optimum methodologies

Because of the non-linear and complex relationship between the input parameters and output parameters, it is quite difficult to select the optimum process parameters for the continuous LTW process. As literature reports, GA is a comprehensive, general-purpose optimization tool which is widely used to solve optimizing problems in the engineering mathematics. It can gather the information depending on the search space in searching process and acquire the optimum relation by managing the searching process adaptively. In the present work, the integrated approach of DF (desirability function)-NSGA-II is used to select the optimum continuous LTW process parameters.

4.1. NSGA-II algorithm

The non-dominated sorting genetic algorithm (NSGA-II) [20], presented by Deb et al., is a fast and elitist multiobjective optimization genetic algorithm for its great performance of global searching. NSGA-II is an evolutionary algorithm of the traditional GA. The mutation operators and crossover remain as usual, but selection operator is different from simple GA. Selection is done with the help of crowded-distance comparison operator, based on ranking (according to non-domination level) and crowding distance. So far, many works [21–24] about optimization have been done, and all these results demostrate that the NSGA-II algorithm is feasible for optimal design.

Table 4
(a) ANOVA analysis for the T_{max} model. (b) ANOVA analysis for the T_{top} model. (c) ANOVA analysis for the *WW* model. (d) ANOVA analysis for the *DT* model.

(a) ANOVA analysis for the T_{max} model.

Source	Sum of squares	df	Mean square	*F*-value	*p*-value
Model	123000	5	24600.3	190.51	< 0.0001
Residual	1870.81	14	129.13		
Cor total	124800	19			

R^2=0.9855 Adjusted R^2=0.9803 Adequate precision=47.816

(b) ANOVA analysis for the T_{top} model.

Source	Sum of squares	df	Mean square	*F*-value	*p*-value
Model	29828.51	5	5965.7	104.78	< 0.0001
Residual	797.07	14	56.93		
Cor total	30625.59	19			

R^2=0.9740 Adjusted R^2=0.9647 Adequate precision=34.388

c) ANOVA analysis for the *WW* model.

Source	Sum of squares	df	Mean square	*F*-value	*p*-value
Model	1.43	7	0.20	103.83	< 0.0001
Residual	0.024	12	0.001967		
Cor total	1.45	19			

R^2=0.9838 Adjusted R^2=0.9743 Adequate precision=36.510

(d) ANOVA analysis for the *DT* model.

Source	Sum of squares	df	Mean square	*F*-value	*p*-value
Model	0.011	3	0.003502	12.24	0.0002
Residual	0.004579	16	0.0002862		
Cor total	0.015	19			

R^2=0.8964 Adjusted R^2=0.8395 Adequate precision=10.539

Table 5
Validation of the established RSM models results.

No.	*P* (W)	*S* (mm/min)	*F* (mm)		T_{max} (°C)	T_{top} (°C)	*WW* (mm)	*DT* (mm)
1	4.1	90	+3	Calculated	351.8	182.6	0.94	0.056
				Predicted	365.2	180.6	0.97	0.060
				Error	3.81%	1.10%	3.19%	7.14%
2	4.65	150	+3	Calculated	327.4	156.1	0.79	0.039
				Predicted	331.7	160.1	0.77	0.041
				Error	1.31%	2.56%	2.53%	5.13%
3	6.1	150	+5	Calculated	364.8	186.7	1.14	0.056
				Predicted	355.2	185.2	1.08	0.061
				Error	2.63%	0.81%	5.26%	8.93%

4.2. Desirability function approach

The basic idea of the desirability function approach is mathematical transformations, by this means, a multiple response problem can transform into a single response problem. The general approach is first to convert each estimated response variable (y_i) into an individual desirability function (d_i), where $0 \le d_i \le 1$, and then the individual desirability functions are combined to obtain the overall desirability of m responses.

The overall desirability *D* is defined by Eq. (7).

$$D = \left[\prod_{i=1}^{m} d_i\right]^{1/m} \tag{7}$$

where $0 \le D \le 1$ and *m* is the number of responses. The optimal solution of the multiple response system is supported by a high value of *D*, which indicates that all individual desirability toward the target value.

According to the following Eqs. (8) and (9), each response y_i can transform to the unitless expected value d_i.

If a response wants to be maximized, the single desirability function can be defined as follows:

$$d_i = \begin{cases} 0 & y_i \le L_i \\ \left(\frac{y_i - L_i}{T_i - L_i}\right)^{wt_i} & L_i < y_i < T_i \\ 0 & y_i \ge T_i \end{cases} \tag{8}$$

The desirability function can be a linear function only when the weight value is equal to 1. When the weight value is greater than 1, it means the function value is closer to the target value, while the weight value is less than 1, it means the target value is less important.

If a response wants to be minimized, the single desirability function can be defined as follows:

$$d_i = \begin{cases} 1 & y_i \le T_i \\ \left(\frac{U_i - y_i}{U_i - T_i}\right)^{wt_i} & T_i < y_i < U_i \\ 0 & y_i \ge U_i \end{cases} \tag{9}$$

where y_i is the response value, L_i is the minimum value of desired response, U_i is the maximum value of desired response and T_i is the target value [25].

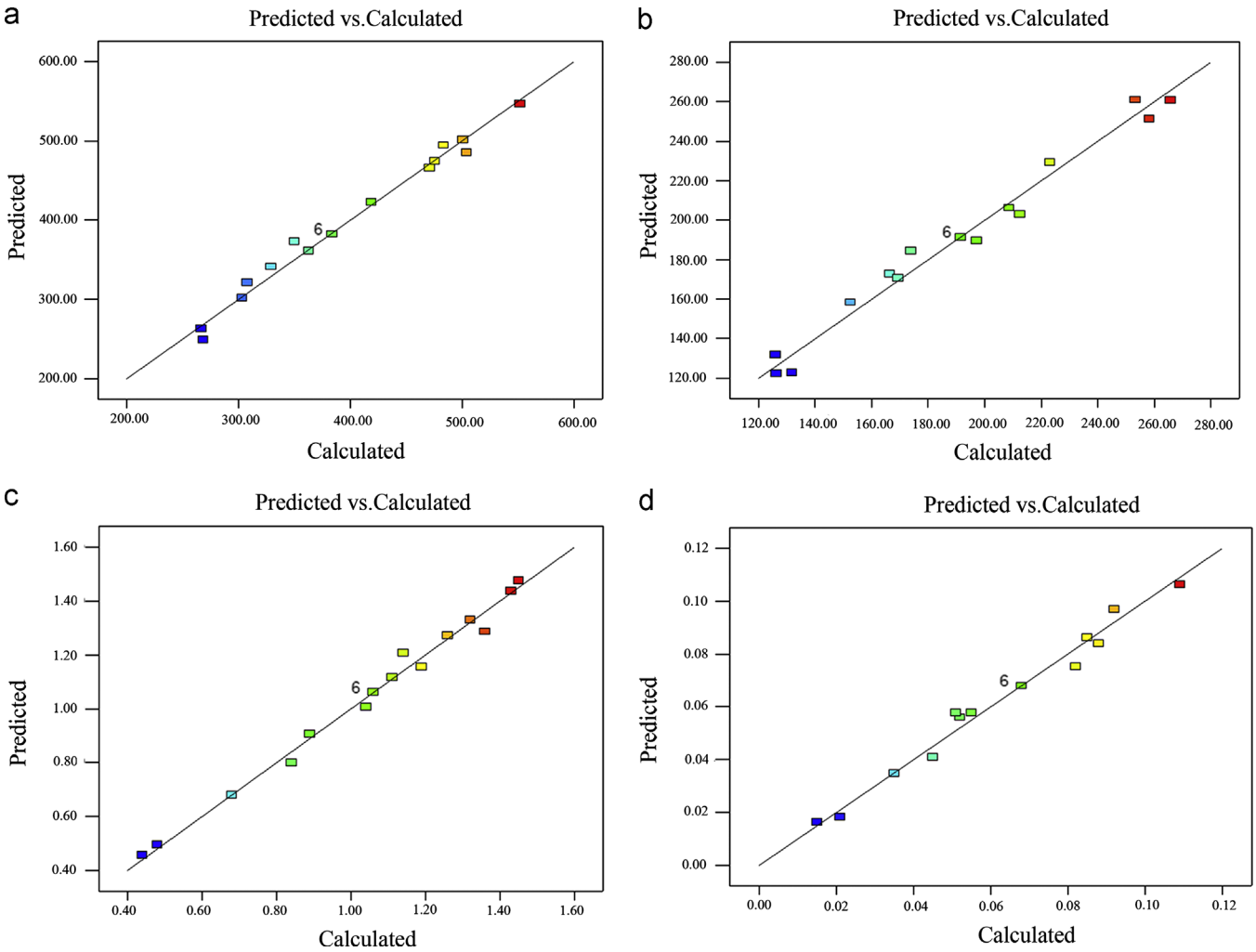

Fig. 14. Plot of calculated vs. predicted response of (a) T_{max} (°C), (b) T_{top} (°C),(c) *WW* (mm), and (d) *DT* (mm) results.

Table 6
Parameters for optimization by desirability function approach.

Response	y_i	L	U	wt	Criteria
T_{max} (°C)	y_1	315	380	1	In range
T_{top} (°C)	y_2	0	252	1	In range

4.3. Results and discussion

In the present study, in order to achieve excellent welding quality, the L of y_i is set as 315.The optimization criterion by method of desirability function is shown in Table 6.

$$D=(d_1\times d_2)^{1/2}\quad d_1=\begin{cases}0 & otherwise\\ 1 & 315^{\circ}C\le y_1\le 380\ ^{\circ}C\end{cases}$$

$$d_2=\begin{cases}0 & otherwise\\ 1 & 0^{\circ}C\le y_2\le 252\ ^{\circ}C\end{cases} \tag{10}$$

The overall desirability can be presented by Eq. (10). In this work, Eq. (10) is used as the fitness function to estimate the suit ability of each individual [26]. The code of NSGA-II optimization using in this work is foating code, the number of initial population is set as 200, maximum iterations of termination function as 'maxGenTerm' are set as 200, the parameter of selection function as 'normGenTerm' is set as 0.08, cross function as 'heuristicXover' is set as (2 3), mutation function as 'multi-NonUnifMutationnon' is set as (6 100 3). Desirability function and genetic algorithm toolboxes of MATLAB 7.0 are used in this study.

Three sets of the optimization data chosen randomly from the whole optimal results and the confirmation tests for validating the optimal results are presented in Table 7.

The results illustrate that the calculated values and the predicted values of the responses are in good agreement with the experiment data each other, which indicate that FEM–RSM–GA–EX approach for producing superior welding quality can be realized, thus the optimized process parameters can be used in confidence.

5. Conclusions

In this study, a particular integrated approach for simulation and optimization of continuous LTW process has been developed through FEM, RSM, GA and experiments. Following conclusions can be drawn from this investigation within the limitations and considerations in this study:

1. A three-dimensional axi-symmetric FE model has been constructed to simulate and analyse the continuous LTW process, and meanwhile the FE model is validated with experimental results.
2. Empirical models can be developed by RSM and confirmed with simulation results with significant accuracy.
3. Optimum continuous LTW process parameters for improving welding quality can be realized with DF and NSGA-II algorithm

Table 7
Verification tests for optimal results.

No.	P (W)	S (mm/min)	F (mm)		T_{max} (°C)	T_{top} (°C)	WW (mm)	DT (mm)
				Calculated	329.1	155.5	0.94	0.044
				Predicted	326.3	151.9	0.92	0.047
				Error	0.85%	2.32%	2.13%	6.82%
1	5.87	187.2	+4.96	Calculated	329.1	155.5	0.94	0.044
				Actual			0.96	0.045
				Error			2.08%	2.22%
				Predicted	326.3	151.9	0.92	0.047
				Actual			0.96	0.045
				Error			4.16%	4.44%
				Calculated	353.4	143.5	0.87	0.046
				Predicted	355.6	143.1	0.83	0.047
				Error	0.62%	0.28%	4.60%	2.17%
2	4.92	175.3	+2.57	Calculated	353.4	143.5	0.87	0.046
				Actual			0.89	0.044
				Error			2.25%	4.55%
				Predicted	355.6	143.1	0.83	0.047
				Actual			0.89	0.044
				Error			6.74%	6.82%
				Calculated	346.4	148.1	0.86	0.045
				Predicted	335.6	137.5	0.81	0.041
				Error	3.12%	7.16%	5.81%	8.89%
3	4.84	180.0	+2.86	Calculated	346.4	148.1	0.86	0.045
				Actual			0.88	0.043
				Error			2.27%	4.65%
				Predicted	335.6	137.5	0.81	0.041
				Actual			0.88	0.043
				Error			7.95%	4.65%

and validated with simulation results, experimental results and empirical model results each other.

The proposed integrated approach (FEM–RSM–GA–EX) is found to provide the admirable optimum performance for the continuous LTW process.

In conclusion, this integrated approach (FEM–RSM–GA–EX) of model establishment has a distinct advantage that it is based on precise FE simulation and can provide an excellent method to choose optimum process parameters for improving efficiency and quality of the continuous LTW process. Last but not the least, the approach will play a commendable guiding role in experiments of LTW process for researchers.

Acknowledgments

The authors acknowledge the National Natural Science Foundation of China (Grant No. 51275219), the Open Foundation of Jiangsu Provincial Key Laboratory of Photon Manufacturing (GZ201105).

Appendix

description

References

[1] Liu Huixia, Wang Kai, Li Pin, Zhang Cheng, Du Daozhong, Hu Yang, et al. Modeling and prediction of transmission laser bonding process between titanium coated glass and PET based on response surface methodology. J Opt Lasers Eng 2012;50(3):440–8.
[2] Wang Xiao, Song Xinhua, Jiang Minfeng, Li Pin, Hu Yang, Wang Kai, et al. Modeling and optimization of laser transmission joining process between PET and 316L stainless steel using response surface methodology. J Opt Laser Technol 2012;44(3):656–63.
[3] Acherjee Bappa, Misra Dipten, Bose Dipankar, Venkadeshwaran K. Prediction of weld strength and seam width for laser transmission welding of thermoplastic using response surface methodology. J Opt Laser Technol 2009;41(8):956–67.
[4] Wang Xiao, Zhang Cheng, Li Pin, Wang Kai, Hu Yang, Zhang Peng, et al. Modeling and optimization of joint quality for laser transmission joint of thermoplastic using an artificial neural network and a genetic algorithm. J Opt Lasers Eng 2012;50(11):1522–32.
[5] Boglea Andrei, Olowinsky Alexander, Gillner Arnold. Fibre laser welding for packaging of disposable polymeric microfluidic-biochips. Appl Surf Sci 2007;254(4):1174–8.
[6] Prabhakaran R, Kontopoulou M, Zak G, Bates PJ, Baylis. B. Laser transmission welding of unreinforced Nylon 6. Soc Plastics Eng 2004;1:1205–9.
[7] Mayboudi LS, Birk AM, Zak G, Bates. PJ. A two-dimensional thermal finite element model of laser transmission welding for T joint. J Laser Appl 2006;18(3):192–8.
[8] Mahmood T, Mian A, Amin MR, Auner G, Witte R, Herfurth H, et al. Finite element modeling of transmission laser microjoining process. J Mater Process Technol 2007;186:7–44.
[9] Mian Ahsan, Mahmood Tonfiz, Auner Greg, Witte Reiner, Herfurth Hans, Newaz Golam. Effects of laser parameters on the mechanical Response of laser irradiated micro-joints. J Mater Research Soc 2006;926:4.
[10] Acherjee B, Kuar A, Mitra S, Mitra D. Finite element simulation of laser transmission welding of dissimilar materials between polyvinylidene fluoride and titanium. J Sci Technol 2010;2(4):176–86.
[11] Acherjee Bappa, Kuar Arunanshu S, Mitra Souren, Misra Dipten. Modeling of laser transmission contour welding process using FEA and DoE. J Opt Laser Technol 2012;44(5):1281–9.
[12] Acherjee Bappa, Kuar Arunanshu S, Mitra Souren, Misra Dipten. Modeling and analysis of simultaneous laser transmission welding of polycarbonates using an FEM and RSM combined approach. J Opt Laser Technol 2012;44(4):995–1006.
[13] Cook R, Malkus D, Plesha M. Concepts and applications of finite element analysis. 3rd ed. New York: John Wiley; 1989.
[14] ANSYS® 12 Manual.
[15] From world wide web. In: www.matweb.com.
[16] Montgomery DC. Design and analysis of experiments. 6th ed. New York: Wiley; 2001.
[17] Design-Expert®, v7, User's Guide, Technical Manual. Minneapolis: Stat-Ease Inc,2007.
[18] Benyounis KY, Olabi AG, Hashmi MSJ. Effect of laser welding parameters on the heat input and weld-bead profile. J Mater Process Technol 2005;164–165:978–85.
[19] Acherjee Bappa, Misra Dipten, Bose Dipankar, Venkadeshwaran K. Prediction of weld strength and seam width for laser transmission welding of thermoplastic using response surface methodology. J Opt Laser Technol 2009;41(8):956–67.
[20] Deb K, Pratap A, Agarwal S, Meyarivan T. A fast and elitist multiobjective genetic algorithm: NSGA-II. J Maga 2002;6(2):182–97.
[21] Mahesh K, Kishore NN, Deb K. Optimal design of composite turbine blade using genetic algorithms. Adv Compos Master 1996;5(2):87–98.
[22] Renner Gabor, Ekart Aniko. Genetic algorithms in computer aided design. J Comput Des 2003;35(8):709–26.
[23] Tran Khoa Duc. Elitist non-dominated sorting GA-II (NSGA-II) as a parameter-less multi-objective genetic algorithm. J Proc IEEE 2005:359–67.
[24] Samad Abdus, Kwang-Yong, Lee Ki-Sang. Multi-objective optimization of a turbomachinery blade using NSGA-II. J San Diego 2007;2:885–91.
[25] Montgomery DC. Design and analysis of experiments. 5th ed. New York: Wiley; 2001.
[26] Pasandideh Seyed Hamid Reza, Niaki Seyed Taghi Akhavan. Multi-response simulation optimization using genetic algorithm within desirability function framework. Appl Math Comput 2006;175(1):366–82.